Soliton formation from a pulse passing the zero-dispersion point in a nonlinear Schrödinger equation

S.R. Clarke, R.H.J. Grimshaw
Department of Mathematics and Statistics
Monash University, Clayton, Victoria 3168, Australia

and

Boris A. Malomed
Department of Interdisciplinary Studies, Faculty of Engineering
Tel Aviv University, Tel Aviv 69978, Israel

February 3, 2008

Abstract

We consider in detail the self-trapping of a soliton from a wave pulse that passes from a defocussing region into a focussing one in a spatially inhomogeneous nonlinear waveguide, described by a nonlinear Schrödinger equation in which the dispersion coefficient changes its sign from normal to anomalous. The model has direct applications to *dispersion-decreasing* nonlinear optical fibers, and to natural waveguides for internal waves in the ocean. It is found that, depending on the (conserved) energy and (nonconserved) "mass" of the initial pulse, four qualitatively different outcomes of the pulse transformation are possible: decay into radiation; self-trapping into a single soliton; formation of a breather; and formation of a pair of counterpropagating solitons. A corresponding chart is drawn on a parametric plane, which demonstrates some unexpected features. In particular, it is found that any kind of soliton(s) (including the breather and counterpropagating pair) eventually decays into pure radiation with the increase of the energy, the initial "mass" being kept constant. It is also noteworthy that a virtually direct transition from a single soliton into a pair of symmetric counterpropagating ones seems possible. An explanation for these features is proposed. In two cases when analytical approximations apply, viz., a simple perturbation theory for broad initial pulses, or the variational approximation for narrow ones, comparison with the direct simulations shows reasonable agreement.

1   Introduction

Nonlinear spatially inhomogeneous waveguides give rise to a number of effects which are of interest by themselves, and also find important applications in such diverse fields as optical *dispersion-decreasing fibers* (DDF) [1] and natural waveguides for internal waves in the ocean with a shear-flow background [2]. It is easy to understand that most nontrivial effects take place in the vicinity of a critical point, where the waveguide's dispersion or nonlinear coefficient changes sign.

The critical points corresponding to the wave propagation of the nonlinear-Schrödinger (NLS) type were classified earlier in Ref. [3], where it was demonstrated that the most interesting one is that at which the sign of the dispersion coefficient α changes. However, unlike the case when the nonlinear coefficient in the corresponding NLS equation changes its sign, this case is not amenable to a consistent analytical consideration, hence systematic numerical simulations are necessary.

In a very recent paper [4], the propagation of a wave pulse in this model was simulated for a situation when α changes its sign, in a self-focussing medium, from anomalous (admitting the existence of bright solitons) to normal (for which bright solitons do not exist). Accordingly, disintegration of an initial soliton-like pulse into radiation wave fields was considered. Despite the apparent simplicity of the process, a number of quite nontrivial features were found and qualitatively explained, the most interesting one being a double-humped structure in the region of the normal dispersion.

For applications, particularly for those related to nonlinear optics of fibers and planar waveguides, especially relevant is the reverse process, i.e., formation of a soliton from a wave pulse crossing into the anomalous-dispersion region from the normal-dispersion one. Previously, this process was considered by one of the present authors in [5] in a purely analytical approximation, based on a variational technique. As we will demonstrate in this work, the system of ordinary differential equations derived in Ref. [5] from the underlying variable-coefficient NLS equation by means of the variational approximation, indeed provides for quite an accurate description of the pulse's dynamics in a parametric region where the approximation is relevant. Nevertheless, most results to be reported in the present work were produced by systematic direct simulations of the NLS equation.

A modified NLS equation, valid near the zero-dispersion point for the nonuniformly guided nonlinear wave propagation, was introduced in the previous works [5, 4]:

$$iu_z + \alpha(z)u_{tt} + 2|u|^2u = i\delta u_{ttt}, \tag{1}$$

where u is the local amplitude of the guided wave, z and t are the distance along the waveguide and the so-called reduced time (see, e.g., the derivation of the corresponding nonlinear Schrödinger equation for optical fibers in the book [6]), $\alpha(z)$ is the above-mentioned sign-changing variable dispersion coefficient, and δ is the third-order-dispersion (TOD) coefficient which, generally, should be included in the case when the usual dispersion becomes very weak [6].

Here we consider solutions to Eq. (1) for a model with a continuous piecewise-

linear dispersion:

$$\alpha(z) = \begin{cases} -1 & z < -1, \\ z & -1 < z < 1, \\ 1 & z > 1, \end{cases} \tag{2}$$

which takes into regard saturation of the dispersion after it has changed sign. This particular configuration can be easily realized in experiments with DDF and, generally, adequately represents the situation that we aim to consider.

We will consider the evolution (for $z > -1$) of a pulse represented by the following natural initial configuration,

$$u(z = -1, t) = A\,\mathrm{sech}(ht). \tag{3}$$

Simulations demonstrate that the evolution of other smooth, *unchirped* initial pulses is very similar to that which is studied in detail below for the initial condition (3).

2 Zero third-order dispersion

If TOD is negligible, Eq. (1) takes a simpler form,

$$iu_z + \alpha(z)u_{tt} + 2|u|^2 u = 0. \tag{4}$$

Both equations (1) and (4) conserve two quantities, viz., the "optical energy"

$$E = \int_{-\infty}^{\infty} |u(z,t)|^2 dt, \tag{5}$$

and the momentum

$$P = \frac{i}{2} \int_{-\infty}^{\infty} (uu_t^* - u^* u_t)dt. \tag{6}$$

These equations admit a Lagrangian representation. In particular, for the simplified equation (4), the *Lagrangian density* is

$$\mathcal{L} = \frac{i}{2}(u^* u_z - uu_z^*) - \alpha(z)|u_t|^2 + |u|^4. \tag{7}$$

Thus for zero TOD and $\alpha(z)$ chosen as per Eqs. (2) and (3), the pulse evolution is governed by the equations

$$iu_z + zu_{tt} + 2|u|^2 u = 0, \qquad (-1 < z < 1) \tag{8a}$$

$$iu_z + u_{tt} + 2|u|^2 u = 0, \qquad (z > 1), \tag{8b}$$

with

$$u(-1, t) = A\,\mathrm{sech}(ht). \tag{8c}$$

The evolution can be characterized by the two parameters, amplitude A and inverse size h of the initial pulse (3), or, alternatively, by its conserved energy

and initial "mass". The "mass", which is *not* a conserved quantity of the NLS equation, is defined as

$$M = \int_{-\infty}^{\infty} |u(z,t)| \, dt. \tag{9}$$

For the initial condition (3), $M_0 \equiv M(z = -1) = \pi A/h$, and $E = 2A^2/h$.

Since dispersion is constant for $z > 1$, the system (8) can be considered as an initial-value problem for the focussing NLS equation, with the initial condition at $z = 1$. Thus the asymptotic solution will consist of a finite number of solitons represented by the discrete spectrum, and dispersive radiation represented by the corresponding continuous spectrum. The number of solitons can be found via the Inverse Scattering Transform for the NLS equation by solving the Zakharov-Shabat (ZS) eigenvalue problem. To this aim, we define

$$q(t) = u(z = 1, t). \tag{10}$$

Assuming that $|q|$ decays as $|t| \to \infty$, the ZS eigenvalue problem is based on the linear equations

$$iv_t - \lambda v = qw, \tag{11a}$$
$$iw_t + \lambda w = \bar{q}v \tag{11b}$$

for auxiliary *Jost functions* u and v, the overbar designating the complex conjugate.

The spectrum of the eigenvalue λ consists of its continuous part on the real axis and discrete eigenvalues, for which nontrivial solutions exist with functions v and w decaying exponentially as $|t| \to \infty$. The number of the discrete eigenvalues in the upper half-plane is then equal to the number of solitons that will evolve from the wave packet $q(t)$. These discrete eigenvalues, in general, have a nonzero imaginary part.

Note that, for a symmetric q, which is the case here, if λ is an eigenvalue, so also is $-\bar{\lambda}$. Solitary purely imaginary eigenvalues then correspond to a single zero-velocity NLS soliton, while multiple ones give rise to stationary *breathers*. If λ has a nonzero real part, then the pair $(\lambda, -\bar{\lambda})$ corresponds to a pair of counter-propagating solitons having velocities of equal magnitude but opposite sign.

Thus, a two-stage process can be used to solve Eqs. (8). Firstly, Eq. (8a) is integrated from $z = -1$ to $z = 1$, using a standard pseudo-spectral in t and fourth-order in z numerical method to obtain $q(t)$ at $z = 1$. This is then used in Eqs. (11) to obtain the characteristics of the discrete spectrum from the ZS eigenvalue problem. Particularly, we want to know the total number of the discrete eigenvalues and the number of discrete eigenvalues on the imaginary axis. These two numbers can be found, using the methods elaborated in Refs. [7] and [8]. Introducing

$$\hat{v} = v \exp(-i\lambda t), \quad \hat{w} = w \exp(i\lambda t), \tag{12}$$

we integrate Eqs. (11) over a finite region $t = [-L, L]$, where $L \gg 1$, using the initial condition $\hat{v}(-L) = 1$ and finding the *transmission coefficient* $\hat{v}(L) = a(\lambda)$. The discrete eigenvalues are then zeros of $a(\lambda)$ in the upper $(\text{Im}\{\lambda\} \geq 0)$ complex

half-plane. Since a is an analytical function of λ, the number of the eigenvalues contained inside a closed curve Γ on the complex plane is

$$N(\Gamma) = \frac{1}{2\pi i} \int_{\Gamma} \frac{a'(\lambda)}{a(\lambda)} d\lambda. \tag{13}$$

To obtain the total number of eigenvalues, let Γ be the curve consisting of the real axis and a semi-circle with an infinitely large radius in the upper half-plane. On this infinite semi-circle, it can be shown that $a(\lambda) \to 1$, thus the total number of eigenvalues is

$$N = \frac{1}{2\pi i} \int_{-\infty}^{\infty} \frac{a'(\lambda)}{a(\lambda)} d\lambda. \tag{14}$$

To obtain the number of discrete eigenvalues lying exactly on the imaginary axis, let Γ_{im} be the perimeter of a vanishingly thin but infinitely long rectangle enclosing the positive imaginary axis. Then the total number of the static (zero-velocity) solitons is $N_{\mathrm{st}} = N(\Gamma_{\mathrm{im}})$.

Before proceeding to full numerical solutions, we can consider two different analytical approximations for a solution of Eq. (8a) in the interval $z = [-1, 1]$, valid, respectively, for long small-amplitude and short large-amplitude pulses. For the long pulses, we define the variables

$$x = ht, \quad u = A\psi. \tag{15}$$

Then (8a) becomes

$$i\psi_z + zh^2\psi_{xx} + 2A^2|\psi|^2\psi = 0, \tag{16a}$$

with

$$\psi(z = -1, x) = \operatorname{sech} x, \tag{16b}$$

Because we now want to consider a long small-amplitude pulse, we assume that $h, A \ll 1$, such that

$$h^2 = \mu, \quad A^2 = \gamma^2\mu, \tag{17}$$

where γ is an $O(1)$ parameter and $\mu \ll 1$. We seek a perturbation solution in the form

$$\psi = (R_0(x) + \mu^2 R_2(z, x) + \dots) \exp\left[i\mu(\phi_1(z, x) + \mu^2\phi_3(z, x) + \dots)\right]. \tag{18}$$

Note that the $O(\mu)$ corrections, R_1 and ϕ_2, can be shown to be identically zero. The initial condition (16b) then gives

$$R_0 = \operatorname{sech}(x). \tag{19}$$

At $O(\mu)$ we obtain

$$R_0\phi_{1z} = zR_{0xx} + 2\gamma^2 R_0^3, \tag{20}$$

and therefore

$$\phi_1 = \frac{1}{2}(z^2 - 1)(1 - 2\operatorname{sech}^2 x) + 2\gamma^2(z + 1)\operatorname{sech}^2 x. \tag{21}$$

Next, at $O(\mu^2)$ it is found that R_2 satisfies the equation

$$R_{2z} = -z(2R_{0x}\phi_{1x} + R_0\phi_{1xx}), \tag{22}$$

and consequently

$$
\begin{aligned}
R_2 = {} & 2\operatorname{sech}^3 x(4 - 5\operatorname{sech}^2 x) \\
& \times \left(\frac{1}{4}(z^4 - 1) - \frac{1}{2}(z^2 - 1) - 2\gamma^2\left(\frac{1}{3}(z^3 + 1) + \frac{1}{2}(z^2 - 1)\right)\right). \tag{23}
\end{aligned}
$$

The amplitude obtained from this perturbation solution is compared with a numerical solution in Fig. 1. As it is seen, the agreement is excellent. This perturbation solution would be expected to be valid for

$$h^2 A^2 \ll 1 \quad \text{or} \quad E \ll 2(M_0/\pi)^{\frac{3}{2}}. \tag{24}$$

In the limit $E \to 0$, while M_0 remains finite, it is apparent that at $z = 1$ the perturbation solution obtained by means of the above method is

$$q(t) \approx A\operatorname{sech}(ht), \tag{25}$$

in which case the variable-dispersion region is simply too short to have any effect on the very long pulse. For this initial condition, a well-known exact solution to the ZS eigenvalue problem was found by Satsuma and Yajima [9]. They showed that the solution consisted of N stationary solitons and a radiative component, where

$$N = \left[\frac{2M_0 + \pi}{\pi}\right], \tag{26}$$

$[\cdot]$ standing for the integer part. For $M_0 = N\pi$, where N is a positive integer, the radiation component is absent, and the solution consists purely of N interacting solitons. Examples of such solutions for $M_0 \gg \pi$ can be found in Ref. [10].

For short pulses, the variational approach proposed in Ref. [5] can be used. To this end, we assume an *ansatz* for the wave packet,

$$u(z, t) = A(z)\operatorname{sech}[t/a(z)]\exp\left[i(\phi(z) + b(z)t^2)\right], \tag{27}$$

where A, a, ϕ and b are slowly varying real functions of z. Varying the averaged Lagrangian,

$$L(z; A, \phi, b, a) = \int_{-\infty}^{\infty}\mathcal{L}\,dt, \tag{28}$$

with respect to these free parameters, it can be shown that A, ϕ and b can be eliminated in favor of the pulse width, a, as

$$\frac{dE}{dz} = \frac{d}{dz}(2aA^2) = 0, \tag{29a}$$

$$b = \frac{1}{4\alpha a}\frac{da}{dz}, \tag{29b}$$

$$\frac{d\phi}{dz} = -\frac{2\alpha}{3a^2} + \frac{5E}{6a}, \tag{29c}$$
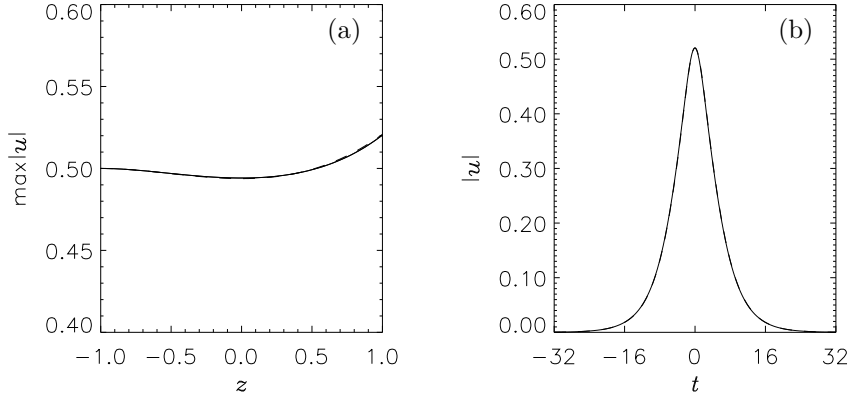
6

Figure 1: A comparison of a numerical solution to Eq. (8) with the perturbation solution (18) for $M_0 = 2\pi$ and $E = 2$, which correspond to $\mu = 1/16$ and $\gamma = 2$ in Eqs. (15) and (17). The numerical solution and perturbation solutions are shown, respectively, by solid and dashed lines (that practically completely coincide). (a) The field $|u|$ at $t = 0$, and (b) $|u|$ at $z = 1$.

where $\alpha(z)$ is the variable dispersion coefficient in Eq. (8a) ($\alpha(z) = z$ in the case under consideration), and $a(z)$ satisfies another variational equation,

$$\frac{d}{dz}\left(\frac{1}{\alpha}\frac{da}{dz}\right) + \left(\frac{4}{\pi}\right)^2\left(\frac{E}{2a^2} - \frac{\alpha}{a^3}\right) = 0. \tag{30}$$

Since the initial chirp is zero, the appropriate initial conditions for (30) are

$$a = h^{-1}, \quad \frac{da}{dz} = 0 \quad \text{at} \quad z = -1. \tag{31}$$

In Fig. 2, an example of a numerical solution to Eqs. (30)–(31) is compared with a full numerical solution of (8). The agreement between the two solutions is quite good, except for a narrow region near the maximum of $|u(t)|$ at $z = 1$. Subsequently, the solutions experience rapid variations with z which the variational ansatz is unable to capture.

Using these analytical approximations and direct numerical solutions, a few different types of the solutions to Eq. (8) can be identified, varying the initial mass and energy of the pulse. The results are summarized in Fig. 3. In the range considered, four particular types of the solutions were found. To construct this diagram, many numerical simulations were required, with particular attention being taken to determine the boundaries between the different regions. Of course, these boundaries can only be determined to the accuracy shown here by using the two-stage numerical process described above. If only direct numerical simulations are used, it becomes very difficult to gauge when a transition occurs. For example, a prohibitively large integration time is needed to distinguish between the decaying-radiation and small-amplitude solitons, whereas this distinction can easily be made by considering the ZS eigenvalue problem.
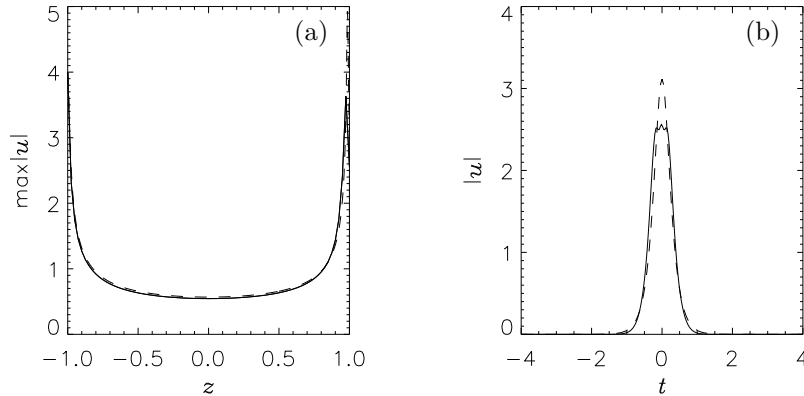
7

Figure 2: A comparison of a numerical solution of Eq. (8) with the variational approximation (27) for $M_0 = \pi/2$ and $E = 4$. The numerical and variational solutions are shown by solid and dashed lines, respectively. (a) The field $|u|$ at $t = 0$, and (b) $|u|$ at $z = 1$.

For a small initial mass M_0, we find no discrete eigenvalues of the ZS scattering problem, so the pulse completely decays into dispersive radiation, in which case $|u|$ has a maximum at $t = 0$ and is monotonically decaying with $|t|$. It is worth noting that near the R–C boundary, a double-humped structure can form at $z > 1$ with symmetric local maxima away from $t = 0$ (which resembles a structure found recently in the same model with the reverse direction of the dispersion change [4]); however, eventually the pulse decays into a monotonically decreasing structure. An example of such a solution in shown in Fig. 4. For $M_0 \to 0$, the evolution of the pulse at $z > 1$ is reasonably well approximated by the solution of the variational equation (30).

As M_0 is increased, two possibilities occur. In the first case, which occurs for small values of E, a single discrete eigenvalue appears on the imaginary axis. This corresponds to the "mass" of the pulse now being sufficiently large to form a soliton. Thus the asymptotic solution consists of a stationary soliton and dispersive radiation, see the example in Fig. 5.

The second case occurs for larger values of E. Here, for sufficiently large values of the initial mass, the chirp has reduced sufficiently for the above-mentioned double-humped structure to develop into a pair of *counter-propagating* solitons. This corresponds to a pair of complex discrete eigenvalues appearing out of the real axis, where $\lambda = \pm\lambda_r + i\lambda_i$, λ_r and λ_i being both real. An example is shown in Fig. 6.

In the last regime, a stationary *breather*, or a bound-state solution forms which asymptotically consists of a pair of interacting solitons. An example of this is shown in Fig. 7. This can happen in two different ways. If the $C \to B$ transition is considered, this occurs when the chirp has reduced sufficiently to no longer cause the splitting of the solitons. In terms of the ZS eigenvalue problem, this corresponds to the two eigenvalues approaching each other at a point on the imaginary axis. After their "collision" on the imaginary axis, two purely
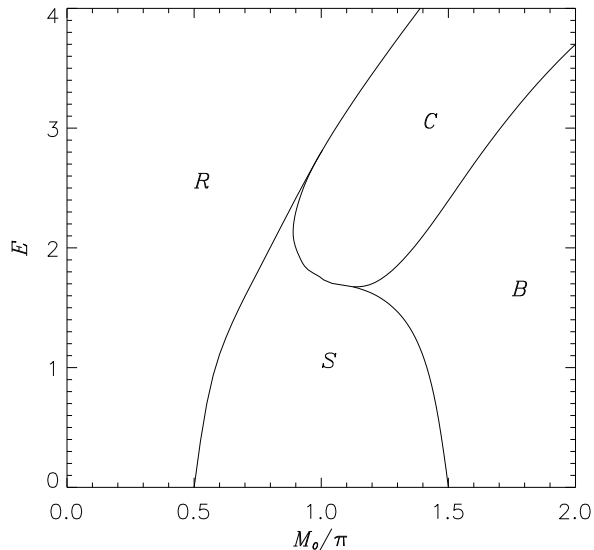
Figure 3: A classification of numerical solutions to Eq. (8) in terms of the energy E and initial mass M_0. R denotes the region of the radiative solutions, S the single-soliton solutions, B the bound-state (breather) solutions, and C the pair of counter-propagating solitons.

imaginary eigenvalues appear, corresponding to two zero-velocity solitons. For the $S \to B$ transition, this simply corresponds to the "mass" having increased sufficiently to give rise to a new zero-velocity soliton. This second soliton, like the one that forms in the $R \to S$ transition, appears out of the origin and corresponds to a purely imaginary eigenvalue.

Within the framework of the ZS eigenvalue problem, generic transitions that lead to the formation of a pair of counter-propagating solitons take place when two eigenvalues appear out of the continuous spectrum, such as occurs for the $R \to C$ transition, or two imaginary eigenvalues collide and subsequently re-shape into a pair of complex eigenvalues, which occurs for the $B \to C$ transition. No evidence has previously been reported of a transition where a single imaginary eigenvalue splits into a pair of complex eigenvalues. Thus, from theoretical considerations, we would expect a B region to always occur between the S and C ones, giving rise to a transition chain $S \to B \to C$. This intermediate B layer must disappear at a *triple point*, where the R and C regions become adjacent, as again the transition $R \to C$ is admitted by the general analysis. For $M_0 > 1.1$ the $S \to B \to C$ transition occurs as expected; however for $M_0 < 1.1$ no evidence of the above-mentioned intermediate B layer could be found. Nevertheless, because a direct splitting of a soliton into a pair of symmetric counterpropagating ones obviously contradicts the principle of continuity and therefore cannot take place in a model governed by a smooth differential equation, we conjecture that the missing intermediate B layer does exist, but it is too thin to be detected using the current numerical techniques.
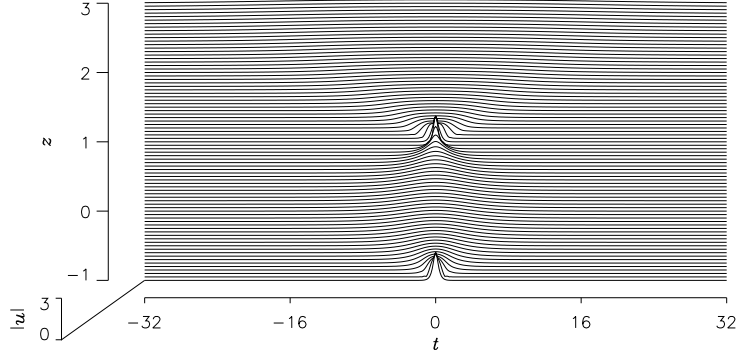
9

Figure 4: The evolution of $|u|$ for a radiative (no-soliton) solution of Eq. (8) with $E = 2$ and $M_0 = \pi/2$.
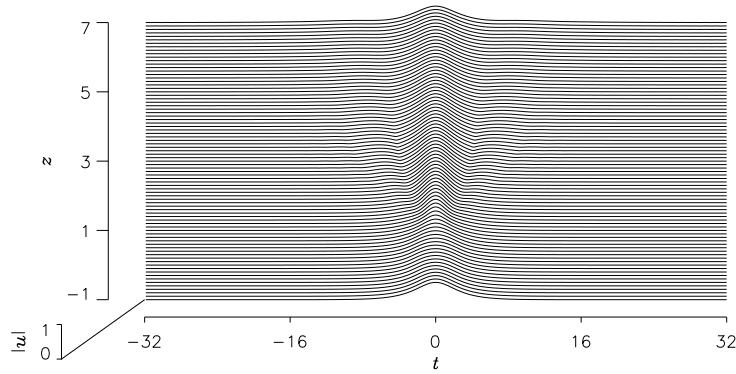

Figure 5: The evolution of $|u|$ for a single-soliton solution of Eq. (8) with $E = 1$ and $M_0 = \pi$. Here, approximately 95% of the energy of the initial pulse is transmitted to the soliton.
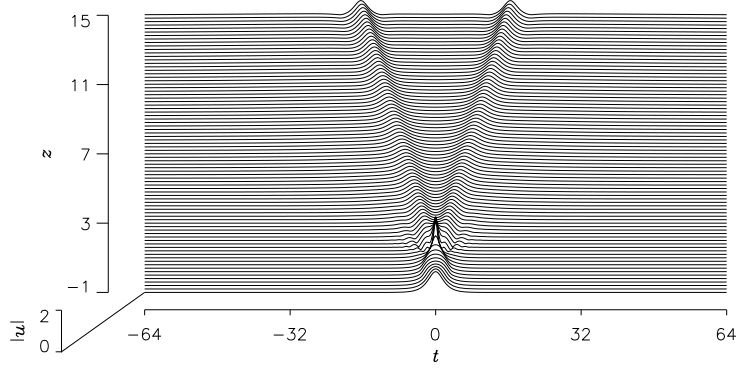
Figure 6: The evolution of $|u|$ for a pair of counter-propagating solitons in Eq. (8) with $E = 3$ and $M_0 = 3\pi/2$. Here, approximately 93% of the energy of the initial pulse is transmitted to the two solitons.
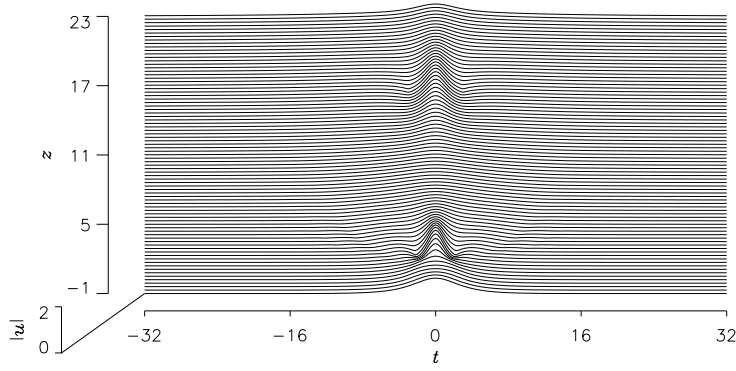

Figure 7: The evolution of $|u|$ for a bound-state (breather) solution of Eq. (8) with $E = 2$ and $M_0 = 3\pi/2$. Here, between 90–95% of the energy of the initial pulse is transmitted to the breather.

11

If the initial "mass" of the pulse is fixed, say, to the value $M_0 = 1$, it is apparent that as the energy is increased the number of solitons goes through the transition $1 \to 2 \to 0$. This result appears counter-intuitive, as one would expect the number of solitons to monotonically increase with the energy. However, this transition can be explained by the influence of the pulse's chirp at $z = 1$. As E is increased, the strength of the chirp increases too. Thus, while for small values of E the chirp may have little effect on the pulse and one soliton is able to form, for larger values of the energy the chirp becomes strong enough to split the single soliton into a pair of solitons [11]. For even larger values of the chirp, this pair is destroyed. A possibility could be to split the two solitons into four moving ones; however, because the mass at $z = 1$ is not sufficient to form four solitons, the pulse decays into radiation.

3   Finite third-order dispersion

In this section, we consider solutions to Eq. (1), supplemented by Eqs. (2) and (3), under the assumption that δ is small ($\delta \ll 1$) but finite. Therefore, the pulse evolution is now governed by the system

$$iu_z + zu_{tt} + 2|u|^2 u = i\delta u_{ttt}, \qquad (-1 < z < 1) \tag{32a}$$

$$iu_z + u_{tt} + 2|u|^2 u = i\delta u_{ttt}, \qquad (z > 1) \tag{32b}$$

with

$$u(z = -1, t) = A \operatorname{sech}(ht). \tag{32c}$$

For $z > 1$, we are again dealing with a constant-coefficient equation, which is, however, no longer integrable (note that this equation, with both constant and periodically modulated coefficient in front of the usual dispersion term, has attracted a lot of attention in nonlinear fiber optics, see, e.g., Refs. [12, 13, 14] and references therein). Thus, only direct numerical simulations can be used to obtain the solutions.

In the consideration of the transition from the anomalous to normal dispersion (i.e., focussing to defocussing), which was the subject of Ref. [4], the pulse width achieved a minimum at the zero-dispersion point $z = 0$, and consequently TOD was becoming more important as this point was approached. However, in the present case the pulse width achieves a *maximum* at $z = 0$ and, in general, a minimum near $z = 1$. Thus, due to the the underlying assumption $|\delta| \ll 1$, it would not be expected that TOD would be significant until well into the focussing (anomalous-dispersion) region. Hence the effect of TOD on the pulse can be estimated by comparing the magnitude of the two constant-coefficient dispersion terms. If the pulse width is $O(a)$, then

$$\left| \frac{\delta u_{ttt}}{u_{tt}} \right| \sim \frac{|\delta|}{a}. \tag{33}$$

From Figs. (4)–(7) it is apparent that, for all the cases, $a_{\min} < h^{-1}$, therefore TOD can be neglected if
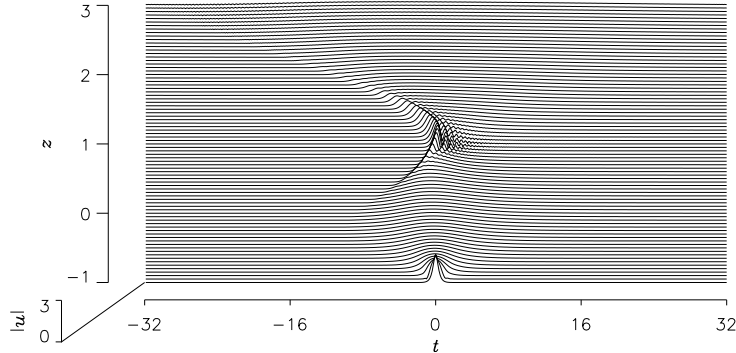
$$|\delta| \ll \frac{2M_0^2}{\pi^2 E}. \tag{34}$$

12

Figure 8: The evolution of $|u|$ for the solution of Eq. (32) with $E = 2$, $M_0 = \pi/2$ and $\delta = 0.01$, demonstrating the effect of the third-order dispersion on the radiative solution which was shown, for the $\delta = 0$ case, in Fig. 4.

When TOD is taken into regard, it manifests itself in three ways. Firstly, TOD destroys the symmetry of the pulse. This is most dramatically seen if one considers the effect of TOD on the radiative solutions, an example of which is shown in Fig. 8 for a small value of the TOD coefficient, $\delta = 0.01$. In the defocussing (normal-dispersion) region $(-1 < z < 0)$, it is apparent that TOD has little effect. However, in the focussing (anomalous-dispersion) region $(z > 0)$, it is apparent that TOD completely destroys the symmetry of the pulse well before the minimum of the pulse width is reached. Comparing this with Fig. 4, it is apparent that, nevertheless, the effect of TOD far away from the zero-dispersion point does not change the radiative type of the solution.

The second effect of TOD, which is now well known, is that solitons are no longer localized, but rather generate a small-amplitude co-propagating oscillatory tail (such nonlocal solitary waves have been termed "nanopterons" by Boyd [15]). Resonant generation of the tails in the context of the modified NLS equation including the TOD term has been considered in several works, see, e.g., Refs. [16, 17]. For a single soliton with speed c and amplitude A, it was demonstrated in Ref. [17] that, for $\delta \ll 1$, the tail has a wavenumber

$$k_r = -\delta^{-1} - c + O(\delta), \tag{35}$$

and amplitude

$$A_r \approx \frac{\pi K}{\delta} \exp\left(-\frac{\pi}{2\delta A}\right), \tag{36}$$

where $K \approx 8.58$. For the single-soliton solutions considered in section 2, the tail generation is a major consequence of TOD (not shown here).

13

The symmetry breaking and appearance of the resonant oscillatory waves are clearly apparent if the effect of TOD on the counter-propagating soliton pair solutions is considered. An example is shown in Fig. 9. With $\delta = 0$, both solitons had the same amplitude and equal but opposite speeds. However, nonzero δ destroys this symmetry. For positive δ, the leftward-propagating soliton is now reduced in amplitude and its speed decreases, whereas for the rightward-propagating soliton the amplitude and speed *increase*. The co-propagating oscillatory waves (tail generation) can be seen both in the evolution of the wave field in Fig. 9(a), and by examining its Fourier transform, which is shown (on the logarithmic scale) in Fig. 9(b) at $z = 15$. For the smaller soliton, the tail can be observed to the right of it, corresponding to the peak in the Fourier transform at $k \approx -3.5$. For the larger soliton, it is more difficult to observe its tail in the evolution plot, however the front of this wave group can be seen starting to propagate rightwards from the pulse at $z \approx 2$. These waves correspond to the well-pronounced peak in the Fourier transform at $k \approx -5.5$

Finally, we consider the effect of TOD on the breather that could exist at $\delta = 0$. In this case, a major effect is *splitting* of the breather into two asymmetric solitons, provided that δ is sufficiently large, an example of which is shown in Fig. 10. Note that a possibility of splitting of a pulse under the action of TOD is also known in the constant-coefficient NLS equation, see, e.g., Ref. [12].

In the case shown in Fig. 10, the main breather-like soliton propagates to the right, but there is also a very weak wave propagating to the left. Whether the leftward-propagating wave is a soliton or just a packet of dispersive radiation cannot be determined. As in Fig. 8, there are oscillatory tail waves co-propagating with the main soliton. The front of these waves can be seen propagating rapidly to the right, and the peak in the Fourier transform at $k \approx -5.3$ (Fig. 10(b)) is associated with these waves. In simulations of the same case, but with $\delta = 0.1$ (twice as small, not shown here), the main breather soliton keeps a nearly zero velocity, and no small-amplitude leftward-propagating wave was detected. Qualitatively, this latter case, with the smaller value of δ, is very similar to what was shown in Fig. 7.

For each of the large-amplitude waves in Figs. (9) and (10), a comparison of the observed co-propagating tail waves can be made with the predictions of Ref. [17], namely the expressions (35) and (36). This is shown in Table (1). For the small-amplitude soliton from Fig. 9, the comparison was not made, as the presence of the soliton with the larger amplitude and its tail renders the asymptotic analysis invalid for the smaller soliton. As can be seen from Table 1 for the dominant rightward propagating soliton, the agreement between the theoretically predicted and observed values of the amplitude is good; however, there is a conspicuous discrepancy, especially in the case shown in Fig. 9, in the values of the wavenumber. Plausibly, the discrepancy can be fixed by including the next-order term in the expansion (35); however, one must also calculate the phase of the solitons in order to do this.

4 Conclusion

In this work, we have analyzed in detail self-trapping of a soliton from a wave packet that passes from a defocussing region into a focussing one in a spatially inhomogeneous nonlinear waveguide, described by a variable-dispersion NLS
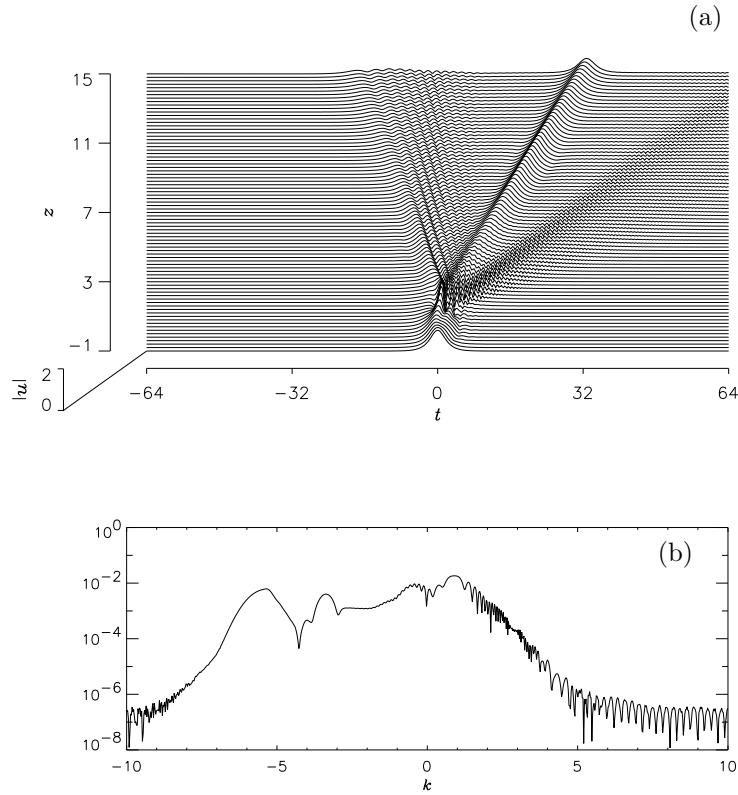
Figure 9: The solution of Eq. (32) with $E = 3$, $M_0 = 3\pi/2$ and $\delta = 0.2$, demonstrating the effect of the third-order dispersion on the counter-propagating soliton-pair solution, which was shown for case $\delta = 0$ in Fig. 6. (a) The evolution of the field $|u|$, (b) the absolute value of the Fourier transform at $z = 15$ (note that the vertical scale in the panel (b) is logarithmic).
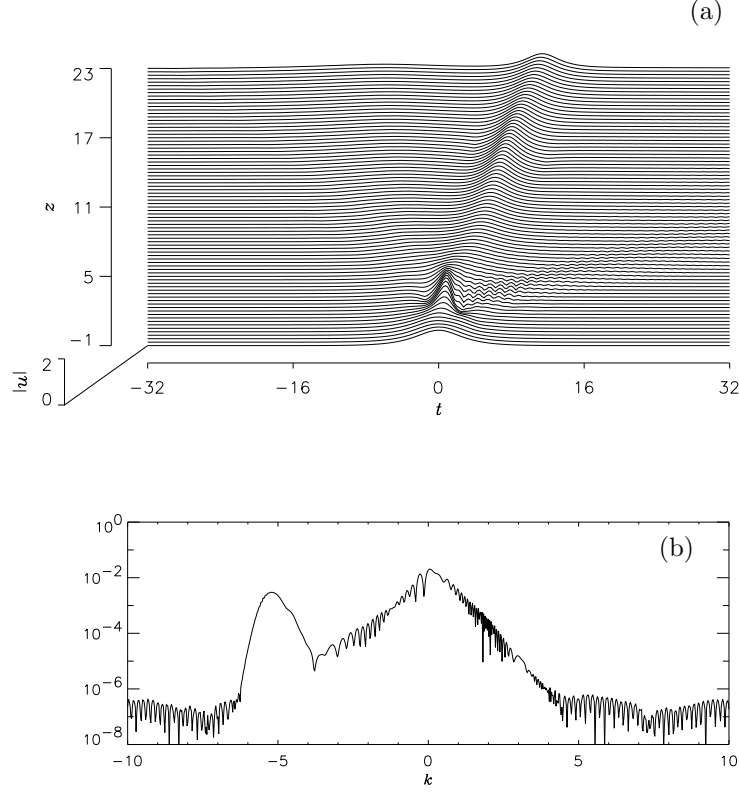
Figure 10: The solution of Eq. (32) with $E = 2$, $M_0 = 3\pi/2$ and $\delta = 0.2$, demonstrating the effect of the third-order dispersion on the bound-state solution shown in Fig. 7. (a) The evolution of the field $|u|$; (b) the absolute value of the Fourier transform at $z = 23$.

Figure	A	c	k_r	A_r	k_o	A_o
(9)	0.8	2.3	-7.3	7×10^{-3}	-5.5	6×10^{-3}
(10)	0.7	0.45	-5.45	2×10^{-3}	-5.3	3×10^{-3}

Table 1: A summary of predicted and observed amplitudes and wavenumbers for the oscillatory tail waves seen in Figs. (9) and (10), where $\delta = 0.2$. A and c are, respectively, the soliton amplitudes and speeds, k_r and A_r are the wavenumbers and amplitudes predicted by Eqs. (35) and (36), while k_o and A_o are the observed ones.

16

equation, in which the dispersion coefficient changes its sign from normal to anomalous. The model can be realized in terms of two (at least) very different but realistic physical applications: a dispersion-decreasing nonlinear optical fiber, and natural waveguides for internal waves in the ocean. It was found that, depending on the values of the (conserved) energy and (nonconserved) "mass" of the initial pulse, four qualitatively different outcomes of the pulse transformation are possible: decay into radiation; self-trapping into a single soliton; formation of a breather; and formation of a pair of counterpropagating solitons. A chart of the corresponding parametric plane has been drawn, which demonstrates some unexpected features. One of them is that, with the increase of the energy, while the initial "mass" is kept constant, a soliton, a pair of the counterpropagating solitons, or a breather eventually decay into pure radiation. Another noteworthy feature is that a direct transition from a single soliton to a pair of symmetric counterpropagating ones seems virtually possible. An explanation for these features was proposed. In two cases when analytical approximations apply, viz., a straightforward perturbation theory for broad initial pulses, or the variational approximation for narrow ones, comparison with the direct simulations shows a good agreement.

Acknowledgements

References

[1] V.A. Bogatyrev et al. A single-mode fiber with chromatic dispersion varying along the length. *J. Lightwave Techn.*, 9:561–566, 1991.

[2] R. Grimshaw. Internal solitary waves. In P.L.-F. Liu, editor, *Advances in Coastal and Ocean Engineering*, volume 3, pages 1–30. World Scientific Publishing Co., 1997.

[3] B.A. Malomed and V.I. Shrira. Soliton caustics. *Physica D*, 53:1–12, 1993.

[4] S.R. Clarke, J. Clutterbuck, R.H.J. Grimshaw, and B.A. Malomed. Passage of a wave pulse through a zero-dispersion point in a nonlinear-schrödinger equation. To appear in *Phys. Lett. E*, 1999.

[5] B.A. Malomed. Formation of a soliton in an inhomogeneous nonlinear wave guide. *Physica Scripta*, 47:797–799, 1993.

[6] G.P. Agrawal. *Nonlinear Fiber Optics*. Academic Press, 1995.

[7] Z.V. Lewis. Semiclassical solutions of the Zakharov-Shabat scattering problem for phase modulated potentials. *Phys. Lett.*, 112A:99–103, 1985.

[8] J.C. Bronski. Semiclassical eigenvalue distribution of the Zakharov-Shabat eigenvalue problem. *Physica D*, 97:376–397, 1998.

[9] J. Satsuma and N. Yajima. Initial value problems of one-dimensional self-modulation of nonlinear waves in dispersive media. *Supp. Prog. Theo. Phys.*, 55:284–306, 1974.

[10] P.D. Miller and S. Kamvissis. On the semiclassical limit of the focussing nonlinear Schrödinger equation. *Phys. Lett. A*, 247:75–86, 1998.

[11] D.J. Kaup, J. El-Reedy, and B.A. Malomed. Effect of a chirp on soliton production. *Phys. Rev. E*, 50:1635–1637, 1994.

[12] M. Desaix, D.A. Anderson, and M.Lisak. Solitons emerging from pulses launched in the vicinity of the zero-dispersion point in a single-mode optical fiber. *Opt. Lett.*, 15:18–20, 1990.

[13] D. Frantzeskakis, K. Hizanidis, B.A. Malomed, and H.E. Nistazakis. Stabilizing soliton transmission by the third-order dispersion in long links with dispersion management. *Pure Appl. Opt*, 7:L57–L62, 1998.

[14] T.I. Lakoba and G.P. Agrawal. Effect of third-order dispersion on dispersion-managed solitons. *J. Opt. Soc. Am. B*, 16:1332–1343, 1999.

[15] J.P. Boyd. *Weakly nonlocal solitary waves and beyond-all-orders asymptotics: generalized solitons and hyperasymptotic theory.* Kluwer Academic Publishers, 1998.

[16] P.K.A. Wai, H.H. Chen, and Y.C. Lee. Radiations by "solitons" at the zero group-dispersion wavelength of single-mode optical fibers. *Phys. Rev. A*, 41:426–439, 1990.

[17] R. Grimshaw. Weakly nonlocal solitary waves in a singularly perturbed nonlinear Shrödinger equation. *Stud. Appl. Math.*, 94:257–270, 1995.